Available online at www.sciencedirect.com
ScienceDirect
Journal of the European Ceramic Society 29 (2009) 1781–1788
www.elsevier.com/locate/jeurceramsoc

Evaluation of the $La_{0.75}Sr_{0.25}Mn_{0.8}Co_{0.2}O_{3-\delta}$ system as cathode material for ITSOFCs with $La_9Sr_1Si_6O_{26.5}$ apatite as electrolyte

Claire Bonhomme [a,b,*], Sophie Beaudet-Savignat [b], Thierry Chartier [a], Pierre-Marie Geffroy [a], Anne-Laure Sauvet [b]

[a] *CNRS-ENSCI, Laboratoire Sciences des Procédés Céramiques et Traitements de Surface (SPCTS), UMR 6638, 47 Avenue Albert Thomas, 87065 Limoges, France*
[b] *Laboratoire de Céramiques et Composants Avancés, CEA Le Ripault, BP 16, 37260 Monts, France*

Received 16 July 2008; received in revised form 21 October 2008; accepted 4 November 2008
Available online 4 January 2009

Abstract

In the past years, a major interest has been devoted to decrease the working temperature of solid oxide fuel cells (SOFCs) down to about 700 °C.

Apatite materials ($La_{10-x}Sr_xSi_6O_{27-x/2}$) are attractive candidates for solid electrolytes, with a high ionic conductivity at 700 °C, a chemical and a dimensional stability for a pO_2 ranging from 10^{-25} to 0.2 atm. A perovskite oxide ($La_{0.75}Sr_{0.25}Mn_{0.8}Co_{0.2}O_{3-\delta}$) has been used as a cathode material.

Symmetrical cathode/electrolyte/cathode cells were fabricated by stacking layers obtained by tape casting of apatite and perovskite powders and co-sintering at 1400 °C for 2 h in air.

Impedance spectroscopy measurements were performed on these cells in order to determine the electrode resistance. It has been shown that the latter decreases with the porosity content of the cathode and with the use of a composite material (apatite/perovskite) instead of a simple perovskite.

Keywords: Tape casting; Composites; Electrical properties; Apatite; Fuel cells

1. Introduction

Lowering the working temperature of a solid oxide fuel cell (SOFC) system down to 700 °C has a great importance to reduce thermal stresses, then to improve the lifetime of the system and to decrease its cost by reducing the price of the interconnector materials. In this respect, the development of new electrolyte and electrode materials with high ionic conductivities at 700 °C is required.

One candidate for the electrolyte material is a ceramic with an apatite structure: $La_9Sr_1Si_6O_{26.5}$. This material has attracted considerable attention because of its high ionic conductivity at 700 °C and its chemical and dimensional stability for a pO_2 varying from 10^{-25} to 0.21 atm.[1–6] Brisse et al.[7] have shown that the electronic transport number of the apatite material $La_9Sr_1Si_6O_{26.5}$ is close to 0, indicating that this material is a pure ionic conductor.

The cathode material is a perovskite oxide $La_{0.75}Sr_{0.25}Mn_{0.8}Co_{0.2}O_{3-\delta}$ which exhibits mixed ionic and electronic conducting properties. The cathode should have an open porosity of 30% for efficient gas transportation and no chemical reactivity with apatite material.

Symmetrical cathode/electrolyte/cathode cells have been fabricated by tape casting of suspensions of $La_9Sr_1Si_6O_{26.5}$ electrolyte and $La_{0.75}Sr_{0.25}Mn_{0.8}Co_{0.2}O_{3-\delta}$ cathode powders, lamination, debinding and co-sintering. The dilatometric behaviors during sintering of the two materials have been adapted by means of the powder characteristics and suspension formulation, in order to prevent cracks, delaminations or deformations during co-sintering. The thermal expansion coefficients (TEC) of the electrolyte and cathode materials are closely matched ($\Delta\alpha = 2.6 \times 10^{-6}\ K^{-1}$), that is necessary to minimize stresses in the co-sintered half-cell.

The aim of this work is first to measure the $La_{0.75}Sr_{0.25}Mn_{0.8}Co_{0.2}O_{3-\delta}$ cathode electrical conductivity and then its resistance on a symmetrical cell, with a $La_9Sr_1Si_6O_{26.5}$ apatite

* Corresponding author at: CNRS-ENSCI, Laboratoire Sciences des Procédés Céramiques et Traitements de Surface (SPCTS), UMR 6638, 47 Avenue Albert Thomas, 87065 LIMOGES, France. Tel.: +33 5 5545 2242; fax: +33 5 5579 0998.
E-mail address: bonhomme_claire@yahoo.fr (C. Bonhomme).

0955-2219/$ – see front matter © 2008 Elsevier Ltd. All rights reserved.
doi:10.1016/j.jeurceramsoc.2008.11.009

material instead of classical yttria-stabilized zirconia as electrolyte.

2. Experimental procedure

2.1. Powder synthesis

The $La_9Sr_1Si_6O_{26.5}$ powder was synthesized using solid-state reaction. Ultra-pure oxide and carbonate precursors, i.e., La_2O_3 (99.99%, Ampère Industrie, France, $d_{50} = 1.5\ \mu m$), SiO_2 (99.99%, Cerac, France, $d_{50} = 22\ \mu m$) and $SrCO_3$ (99.99%, Alfa Aesar, France, $d_{50} = 4.3\ \mu m$) were used. The mixture of the three powders was attrition-milled using 0.8-mm-diameter zirconia balls in water for 3 h 30 min, dried and calcined at 1400 °C for 4 h. Then, the synthesized powder was attrition-milled in alcohol using a dispersant (phosphate ester, 1 wt% on the powder base). Attrition milling was stopped when the particle size reached a monomodal distribution with a mean particle size of 0.75 μm (laser granulometer—Mastersizer 2000, Malvern Instruments). Finally, the suspension was dried.

The $La_{0.75}Sr_{0.25}Mn_{0.8}Co_{0.2}O_{3-\delta}$ powder was provided by Praxair, USA ($d_{50} = 0.75\ \mu m$). The perovskite powder was calcined at 1150 °C for 2 h in order to adapt its sintering reactivity to the apatite powder with the objective of co-sintering. After calcination, the perovskite powder has a bimodal particle size distribution centered respectively on 1.2 μm and 9.5 μm.

2.2. Samples preparation

The gas-tight $La_9Sr_1Si_6O_{26.5}$ apatite ceramic and the porous layers of $La_{0.75}Sr_{0.25}Mn_{0.8}Co_{0.2}O_{3-\delta}$ perovskite were elaborated by tape casting.

The first step in the preparation of a tape casting suspension consisted in the dispersion of the ceramic powder in a solvent. This was performed by planetary ball milling with alumina balls during 1 h in MEK–ethanol (60/40) containing 1.5 wt% of a phosphate ester dispersant. Then, an acrylic binder and a phthalate plasticizer were added to the suspension and mixed during 16 h. The binder is probably the most important processing additive. It confers the mechanical properties to the green sheets and also controls the rheology of the suspension. The plasticizer improves the flexibility and enables the green tape to be manipulated and punched without cracking.[8] The optimum concentrations for the binder and plasticizer were determined to be 10.8 wt% for both additives on the base of the ceramic powder for the electrolyte and 8 wt% for the cathode.

The porous structure of the cathode was obtained by introducing a pore forming agent (PFA) in the perovskite tape casting suspension. Fifteen micrometers mean diameter corn-starch particles were used as PFA because of their narrow particle size distribution and their total combustion during the thermal treatment. PFA volume fractions of 42.2% and 49.7% (on the base of the ceramic powder) were used in order to obtain an interconnected porosity. A subsequent 4 h mixing time led to a uniform distribution of the PFA in the suspension.

Finally, the suspensions were de-aired at a low rotating speed during 48 h before being tape-casted onto a plastic film using a moving double blade device on a laboratory tape casting bench.

After drying, the green tape thickness was 260 μm for the electrolyte and 95 μm for the cathode. Thirty millimeter-diameter disks were then punched in the green tapes.

A symmetrical cathode/electrolyte/cathode cell was elaborated by stacking five electrolyte layers and two cathode layers on each side of the electrolyte. The stacks were then laminated under 40 MPa at 85 °C. The organics introduced in the tape casting suspensions were burn out by slow heating rate (0.3 °C/min) in air up to 600 °C. Co-sintering of the symmetrical cathode/electrolyte/cathode cell was performed in air during 2 h at 1400 °C with a 5 °C/min heating rate.

Conductivity tests on cathode materials were performed on rectangular green compacts with nominal dimensions 5mm × 5mm × 50mm, prepared by uniaxially pressing the perovskite powder under 100 MPa. A porous sample was obtained by mixing a PFA volume fraction of 49.7% with the perovskite powder. The compacts were then sintered in air at 1400 °C for 2 h, with a 5 °C/min heating rate.

2.3. Structural and microstructural analyses

The densification kinetics and the final shrinkages of the electrolyte and cathode were controlled by dilatometric measurements performed on green tape-casted materials in air at 1400 °C with a 2-h dwell-time (dilatometer DI24, ADAMEL, LHOMARGY).

The densities of the sintered materials were measured using the Archimedes method. Microstructures were observed by S.E.M. (S-2500, Hitashi) on polished cross-sections after a thermal etching of grain boundaries.

The eventual interface reactions between $La_9Sr_1Si_6O_{26.5}$ and $La_{0.75}Sr_{0.25}Mn_{0.8}Co_{0.2}O_{3-\delta}$, after co-sintering, were verified by EDS on fractured sections.

2.4. Electrical and electrochemical characterizations

The electrical conductivity of the dense and porous sintered cathode samples was measured in air by standard four-probe DC techniques. Measurements were performed from room temperature to 1000 °C at a rate of 5 °C/min. A direct current of 100 mA was passed through the two outside terminals, and the voltage was measured between the two inside terminals.

Electrochemical measurements on symmetrical cathode/electrolyte/cathode cells were carried out using AC impedance spectroscopy. The measurements were performed in air between 300 °C and 800 °C, with a 30 mV signal amplitude at open circuit voltage in the 10^{-3}–10^{6} Hz frequency range. Nyquist diagrams obtained were fitted using Zview software.[9]

3. Results and discussion

3.1. Elaboration of a symmetrical cathode/electrolyte/cathode cell

Dilatometric measurements were performed on green tape-casted electrolyte and cathode materials (Fig. 1).

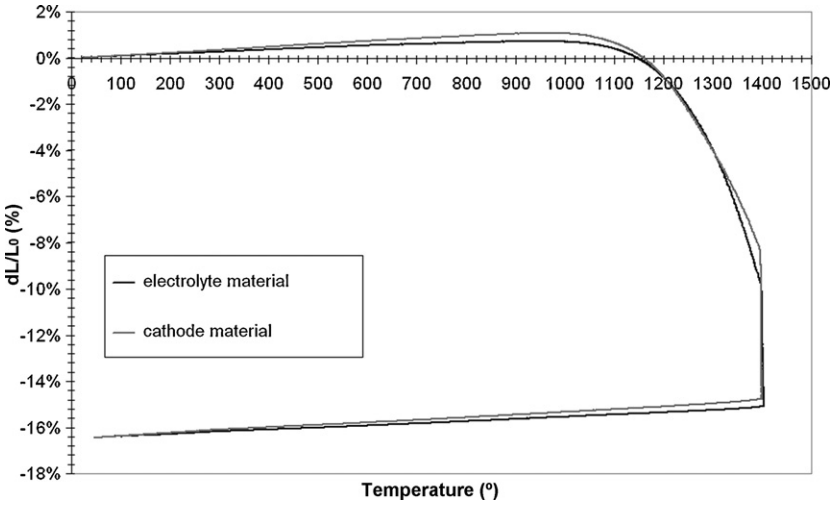

Fig. 1. Dilatometric curves during sintering of the $La_{0.75}Sr_{0.25}Mn_{0.8}Co_{0.2}O_{3-\delta}$ cathode (PFA volume fraction of 49.7%) and the $La_9Sr_1Si_6O_{26.5}$ electrolyte materials, in air, at 1400 °C for 2 h.

The densification kinetics and the final shrinkages of the electrolyte and cathode are close, that is critical to avoid deformation and cracking of the symmetrical cell during the sintering process.

Symmetrical cathode/electrolyte/cathode cells, with cathode of two porous volumes (35.8% and 42.7%), were then co-sintered in air at 1400 °C–2 h (Fig. 2). The thickness is about 760 μm for the dense electrolyte and 92 μm for the ex-corn-starch porous cathodes.

No delamination was observed at the interface of electrolyte and cathode materials (Fig. 2).

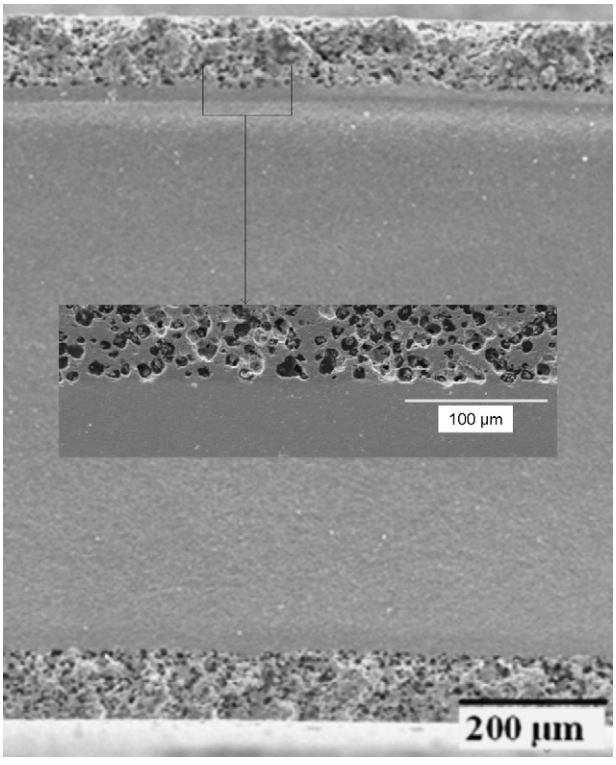

Fig. 2. Cross-section of the cathode/electrolyte/cathode cell (cathode porosity = 35.8%) and zoom on the interface between electrolyte and cathode materials.

EDS analysis revealed no diffusion of the perovskite elements (Co, Mn) in the apatite structure (Fig. 3). However, La, Sr and O diffusion between apatite ($La_9Sr_1Si_6O_{26.5}$) and perovskite ($La_{0.75}Sr_{0.25}Mn_{0.8}Co_{0.2}O_{3-\delta}$) cannot be neglected because these elements are present in both materials. Further analyses could be necessary to determine more precisely this diffusion.

3.2. Electrical and electrochemical properties of the $La_{0.75}Sr_{0.25}Mn_{0.8}Co_{0.2}O_{3-\delta}$ perovskite material

3.2.1. Electrical conductivity of the $La_{0.75}Sr_{0.25}Mn_{0.8}Co_{0.2}O_{3-\delta}$ perovskite material

Fig. 4 shows the electrical conductivity plots ($\log \sigma T$) versus inverse temperature for a dense and a 42.7% porous perovskite samples, measured from room temperature to 1000 °C in air.

The cathode $La_{0.75}Sr_{0.25}Mn_{0.8}Co_{0.2}O_{3-\delta}$ is a good electronic conductor ($\sigma = 113$ S/cm at 700 °C) and its conductivity is logically decreasing with the introduction of porosity ($\sigma = 45$ S/cm at 700 °C).

As the ionic transport value in this composition is less than 1%,[10] the bulk conductivities obtained by dc four terminal measurements are representative of the electronic conductivity, with a mean activation energy of 0.15 eV.

3.2.2. Electrochemical properties of a symmetrical cathode/electrolyte/cathode cell

3.2.2.1. Influence of the cathode porous volume. Impedance spectroscopy measurements were performed on symmetrical cathode/electrolyte/cathode cells, with cathode of two porous volumes (35.8% and 42.7%) (Fig. 5).

The Nyquist diagrams behaviors are similar for the two symmetrical cells with a similar frequency distribution. The electrode resistance is lower for the more porous cathode.

The kinetic of O_2 reduction on a mixed-conducting electrode has been treated by the Adler–Lane–Steele (ALS) model.[11–14]

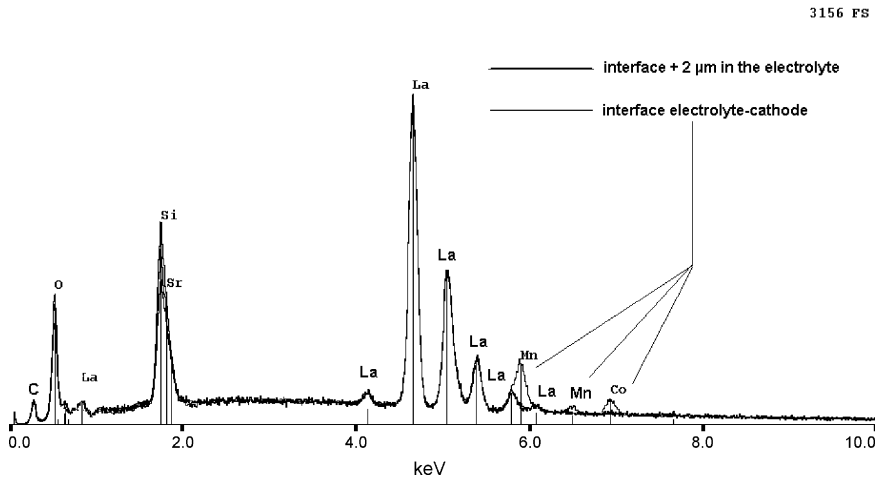

Fig. 3. EDS analyses at the interface of $La_9Sr_1Si_6O_{26.5}$ apatite and $La_{0.75}Sr_{0.25}Mn_{0.8}Co_{0.2}O_{3-\delta}$ perovskite materials and in the apatite material at 2 μm from the interface.

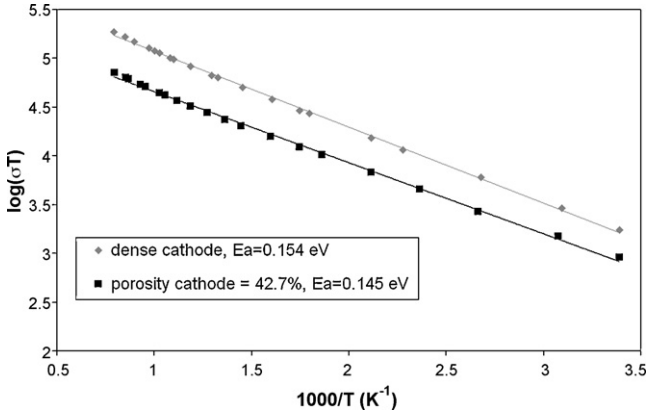

Fig. 4. Temperature dependence of the electrical conductivity for a dense and a 42.7% porous cathode materials.

In this model, the electrode reaction

$$(1/2)O_2 + 2e^- \rightarrow O^{2-} \quad (1)$$

is assimilated to the conversion of an electronic current to an ionic one over the cathode thickness.

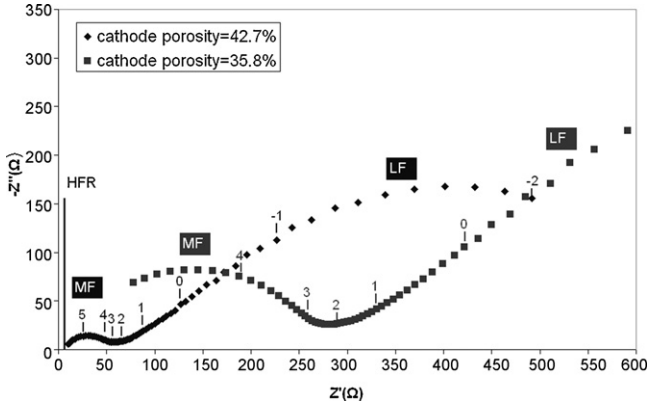

Fig. 5. Nyquist diagram at 700 °C of symmetrical $La_{0.75}Sr_{0.25}Mn_{0.8}Co_{0.2}O_{3-\delta}$/$La_9Sr_1Si_6O_{26.5}$/$La_{0.75}Sr_{0.25}Mn_{0.8}Co_{0.2}O_{3-\delta}$ cells sintered at 1400 °C–2 h. The logarithm of the relaxation frequencies is reported on the diagram.

The impedance of a symmetrical cell can be expressed as

$$Z = R_{\text{electrolyte}} + Z_{\text{interfaces}} + Z_{\text{chem}} \quad (2)$$

where $R_{\text{electrolyte}}$ is the electrolyte resistance, $Z_{\text{interfaces}}$ the impedance of the electron-transfer and ion-transfer processes occurring at the current collector/electrode and electrolyte/electrode interfaces respectively and Z_{chem} includes oxygen surface exchange, solid-state diffusion of O^{2-} and gas-phase diffusion inside and outside the electrode.

The electrode resistance is constituted by two semicircles, the first at middle frequency (MF) and the other one at lower frequency (LF). The aim of the study is to verify if MF and LF contributions correspond to those proposed in the ALS model ($Z_{\text{interfaces}}$ and Z_{chem} respectively).

The Nyquist diagram in Fig. 5 can be fitted on the basis of an equivalent circuit constituted of electrical elements associated with a specific electrochemical process: a high frequency resistance (HFR), in series with two parallel elements (R//CPE) (Fig. 6).

According to the ALS model, the high frequency intersection HFR (Fig. 5) should correspond to the electrolyte resistance. The evolution of the conductivity with temperature calculated from HFR for the symmetrical cells is compared to the electrolyte one in Fig. 7.

The conductivity values, calculated from the resistance HFR, close to the electrolyte $La_9Sr_1Si_6O_{26.5}$ one, confirm that the HFR could be attributed to the ohmic loss of the electrolyte.

The impedance response of the electrode is observed in the frequency range 10^{-2} to 10^6 Hz (Fig. 5).

The mean capacitance (CPEMF) of the middle frequency contribution has been calculated as 1.2×10^{-8} F/cm^2 and 6×10^{-9} F/cm^2 respectively for the 35.8% and 42.7% porous

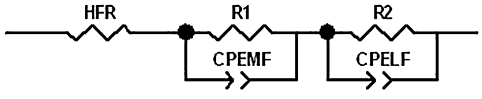

Fig. 6. Equivalent circuit accounted for the electrochemical response of the symmetrical cells.

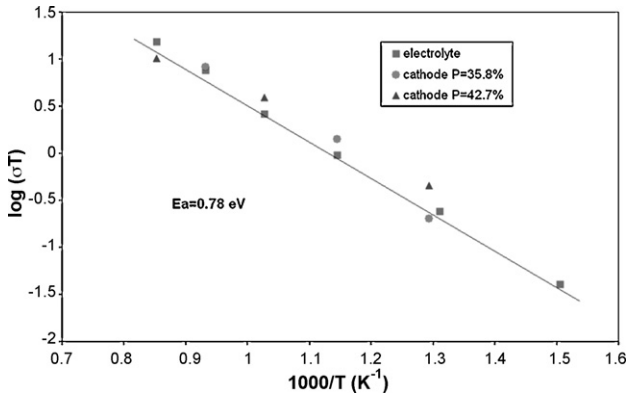

Fig. 7. Arrhenius diagram of the high frequency resistance (HFR) of the symmetrical cells, compared to the electrolyte one.

cathode. In previous studies on $Nd_{1.95}NiO_4$/YSZ/$Nd_{1.95}NiO_4$ symmetrical cells,[15] a similar middle frequency arc has also been observed with a capacitance of the same order of magnitude. This arc has been assigned to the electrode/electrolyte charge-transfer reaction. So, the resistance R_1 could correspond to the ionic-transfer resistance occurring at the interface.

The values of R_1 decrease with temperature (Fig. 8), which means that the ionic transfer at the interface electrolyte/electrode is a thermally activated process.

The low frequency contribution LF (R2//CPELF) has a mean capacitance of 10^{-2} F/cm^2. According to previous studies,[14] this arc could be assigned to the chemical impedance (Zchem in the ALS model) associated with non-charge-transfer processes occurring in the electrode.

The electrode resistance is lower for the cathode containing a porosity of 42.7% indicating better gas-phase diffusion inside the more porous cathode material and/or a better absorption of O_2 molecules. As the cathode material is a mixed ionic and electronic conductor, the triple phase boundary surface is increasing with the porous volume, resulting also in a decrease of the charge-transfer resistance.

However, the electrode resistance remains high and some improvements concerning the cathode material are required in order to increase its catalytic activity for oxygen reduction. Firstly, the cobalt content could be increased in the

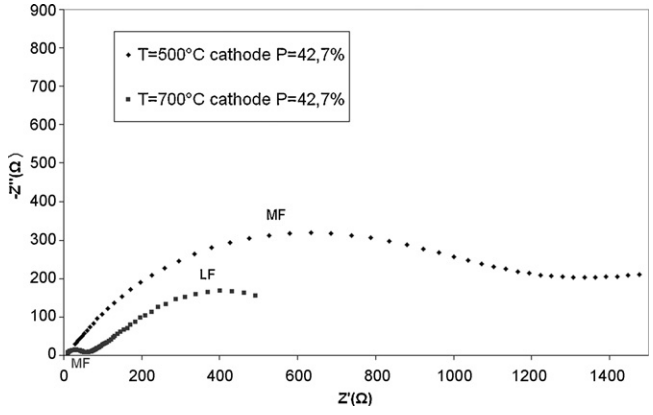

Fig. 8. Evolution of the middle frequency contribution with temperature for the symmetrical cell containing a 42.7% porous cathode.

perovskite material in order to enhance its ionic conductivity. However, it has been shown that increasing the cobalt content leads to an increase of the thermal expansion coefficients of perovskite materials (for instance, the TEC of the $La_{0.6}Sr_{0.4}Mn_{0.2}Co_{0.8}O_{3-\delta}$ composition is equal to 18.2×10^{-6} K^{-1})[10]. Then, the mismatch of thermal expansion coefficients between the apatite and perovskite is increasing, leading to stresses and risks of delaminations. In this respect, this solution could not be retained. Secondly, a composite cathode consisting of a mixture of perovskite and apatite materials could be elaborated in order to increase the triple phase boundary surfaces. In this case, the reduction of oxygen is extended on the whole electrode volume.[16–18]

3.2.2.2. Composite cathode material. A composite cathode is consisting in a mixture of the ionic conducting apatite and the mixed-conducting perovskite. The perovskite powder $La_{0.75}Sr_{0.25}Mn_{0.8}Co_{0.2}O_{3-\delta}$ provides the electronic pathways and catalyzes the formation of surface oxygen species O^{2-}. These oxygen species are then injected into the apatite particles which transport most of the ionic flux to the cathode/electrolyte interface. The apatite/perovskite volume ratio should be adapted in order to establish parallel conduction paths for ions and electrons within the cathode material.[19]

Using a composite cathode presents some advantages. Firstly, the chemical compatibility between the electrolyte and cathode materials is enhanced. Secondly, the thermal expansion coefficient mismatch between electrolyte and cathode materials is reduced, improving their adherence during the cell operation.[20–22]

The electrode–electrolyte volume ratio has been chosen at 50:50 because it has been shown that the minimum charge-transfer resistance is achieved for this volume ratio.[23] For the fabrication of the composite cathode, the apatite and perovskite powders were mixed in stoichiometric proportions and a tape casting suspension was elaborated. A PFA volume fraction of 49.9% was used.

The symmetrical composite cathode/electrolyte/composite cathode cell was then co-sintered in air at 1400 °C for 2 h. Fig. 9 shows a S.E.M. microstructure of the composite cathode, correlated with EDS analyses.

According to EDS analyses, the light-gray particles correspond to apatite phase and the dark-gray particles to the perovskite phase. Both ionic and electronic conduction paths are provided in the composite cathode material.

Impedance spectroscopy measurements were performed on the symmetrical composite cathode/electrolyte/composite cathode cell and compared to the $La_{0.75}Sr_{0.25}Mn_{0.8}Co_{0.2}O_{3-\delta}$/$La_9Sr_1(SiO_4)_6O_{2.5}$/$La_{0.75}Sr_{0.25}Mn_{0.8}Co_{0.2}O_{3-\delta}$ one (Fig. 10).

The use of a composite cathode in a symmetrical cell leads to a decrease by a factor of 5 of the cathode resistance ($R = 31\ \Omega/cm^2$ at 700 °C).

The evolution of the conductivity calculated from HFR for the symmetrical cell is almost the same as the electrolyte one. So, the high frequency resistance could be assimilated as the electrolyte resistance.

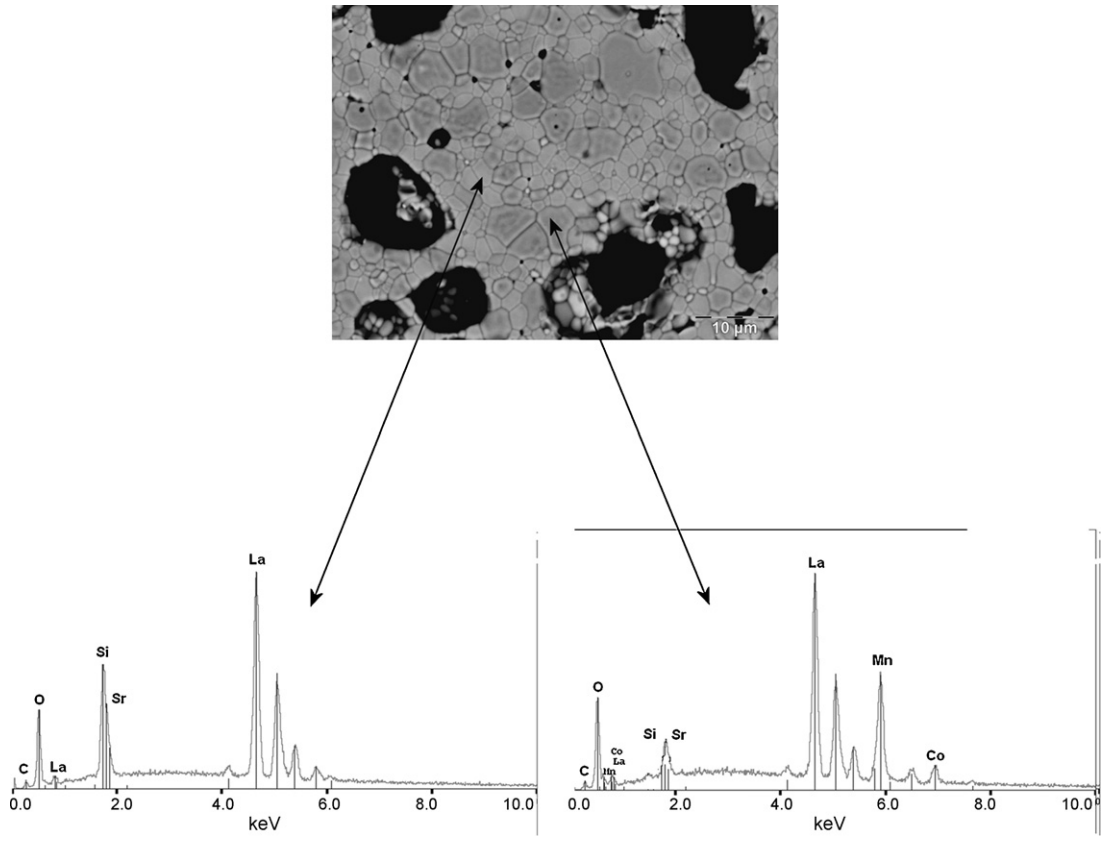

Fig. 9. Microstructure of the composite cathode associated with EDS analyses (a) on a light-gray particle and (b) on a dark-gray particle.

The impedance response of the composite electrode is observed in the frequency range 10^{-2} to 10^{4} Hz.

According to the capacitance values for each arc (1.10^{-2} F/cm^2 for the LF contribution and 1.10^{-5} F/cm^2 for the MF contribution, Fig. 11) and with respect to previously reported values for other cathode materials,[14,22,24,25] the arc located in the middle frequency range could originate from the ionic transfer occurring at the electrode/electrolyte interface, and the low frequency arc may be due to non-charge-transfer processes occurring in the electrode material.

In order to determine the rate-determining step in the oxygen reduction reaction, a further study would consist in using the slope of the electrode resistance as a function of oxygen partial

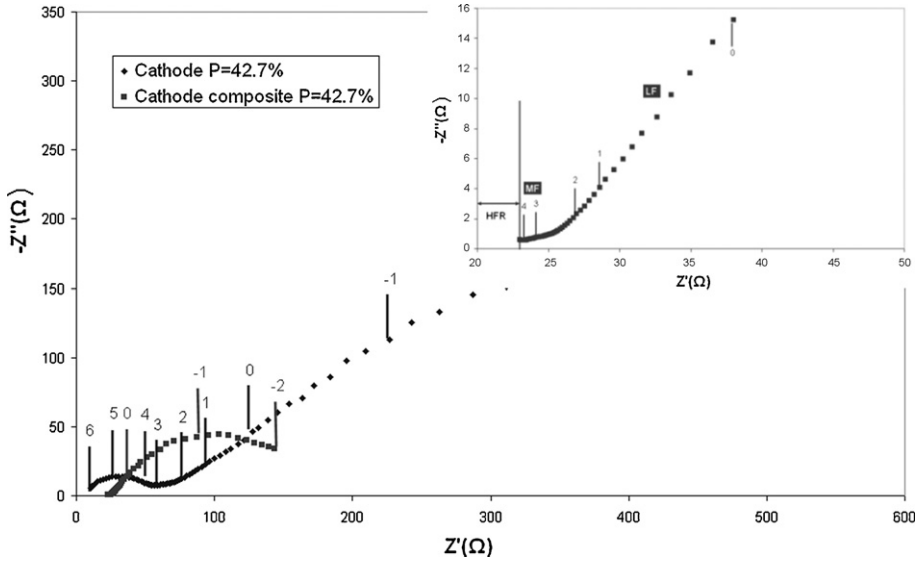

Fig. 10. Nyquist diagrams between two symmetrical $La_{0.75}Sr_{0.25}Mn_{0.8}Co_{0.2}O_{3-\delta}/La_9Sr_1(SiO_4)_6O_{2.5}/La_{0.75}Sr_{0.25}Mn_{0.8}Co_{0.2}O_{3-\delta}$ and composite cathode/$La_9Sr_1(SiO_4)_6O_{2.5}$/composite cathode cells at 700 °C.

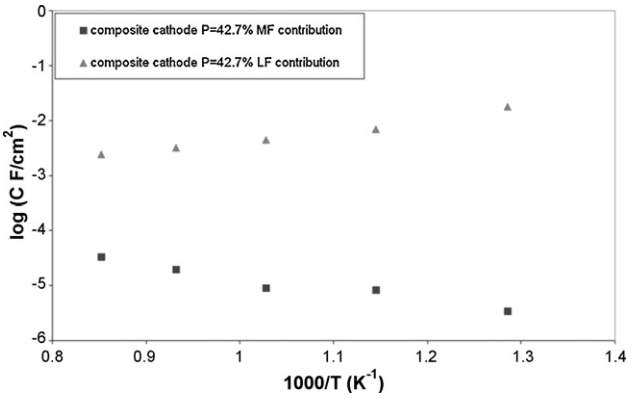

Fig. 11. Thermal dependence of the capacitance for the composite cathode deposited on apatite electrolyte.

pressure, according to the relation:

$$\frac{1}{R_p} \propto P_{O_2}^m \quad (3)$$

The m value would give information about the species involved in the electrode reaction.[26]

Concerning the composite cathode, the conductivity of the MF and LF contributions are thermally activated and the activation energy calculated from the Arrhenius diagram is lower for the middle frequency contribution (0.93 eV) than for the low frequency one (1.33 eV) (Fig. 12).

Furthermore, the conductivity of the MF contribution is raising with the use of a composite cathode, suggesting that the ionic transfer at the interface electrolyte/cathode is enhanced.

Finally, when a symmetrical cell is constituted by a composite cathode, the triple phase boundary surface is increased through the whole volume of the cathode material, leading to a more important ionic flux towards the electrode/electrolyte interface.

Some improvements are currently in progress in order to still decrease the electrode resistance, for instance by reducing the cathode thickness to make easier the gas progress towards the interface.

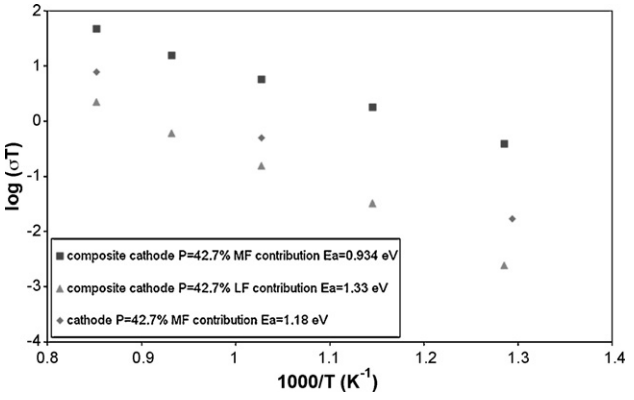

Fig. 12. Arrhenius plots of the conductivity of composite cathodes deposited on apatite electrolyte and comparison of the MF contribution for composite and classical electrodes.

4. Conclusion

Electrical and electrochemical analyses have been performed on cathode and on symmetrical cathode/electrolyte/cathode cells. These materials were elaborated by tape casting and co-sintering at 1400 °C–2 h in air.

Neither delamination nor reactivity between apatite and perovskite materials has been observed. The electrode resistance, measured by impedance spectroscopy, decreased with an increase of the cathode porosity content and with the use of a composite cathode material, leading to an enhancement of the triple phase boundary surface through the cathode material.

The electronic conductivity of the $La_{0.75}Sr_{0.25}Mn_{0.8}Co_{0.2}O_{3-\delta}$ perovskite material, measured by a standard four-probe DC technique, is equal to 113 S/cm.

References

1. Nakayama, S. and Sakamoto, M., Electrical properties of new type high oxide ionic conductor $RE_{10}Si_6O_{27}$ (RE = La, Pr, Nd, Sm, Gd, Dy). *J. Eur. Ceram. Soc.*, 1998, **18**, 1413–1418.
2. Nakayama, S. and Highchi, M., Electrical properties of apatite-type oxide ionic conductors $RE_{9.33}(SiO_4)_6O_2$ (RE = Pr, Nd and Sm) single crystals. *J. Mater. Sci. Lett.*, 2001, **20**, 913–915.
3. Nakayama, S., Kageyama, T., Aono, H. and Sadaoka, Y., Ionic conductivity of lanthanoid silicates, $Ln_{10}(SiO_4)_6O_3$ (Ln = La, Nd, Sm, Gd, Dy, Y, Ho, Er and Yb). *J. Mater. Chem.*, 1995, **5**, 1801–1805.
4. Leon-Reina, L., Losilla, E. R., Martinez-Lara, M., Bruque, S. and Aranda, M. A. G., Interstitial oxygen conduction in lanthanum oxy-apatite electrolytes. *J. Mater. Chem.*, 2003, **14**, 1142–1149.
5. Sansom, J. E. H., Richings, D. and Slater, P. R., A powder neutron diffraction study of the oxide-ion-conducting apatite-type phases, $La_{9.33}Si_6O_{26}$ and $La_8Sr_2Si_6O_{26}$. *Solid State Ionics*, 2001, **139**, 205–210.
6. Arikawa, H., Nishiguchi, H., Ishihara, T. and Takita, Y., Oxide ion conductivity in Sr-doped $La_{10}Ge_6O_{27}$ apatite oxide. *Solid State Ionics*, 2000, **136–137**, 31–37.
7. Brisse, A., Sauvet, A. L., Barthet, C., Georges, S. and Fouletier, J., Microstructural and electrochemical characterizations of an electrolyte with an apatite structure, $La_9Sr_1Si_6O_{26.5}$. *Solid State Ionics*, 2007, **178**, 1337–1343.
8. Chartier, T., Ceramic forming processes. In *Ceramic materials—processes, properties and applications*, ed. P. Boch and J. C. Niepce, 2007 (Chapter 5).
9. Derek, J., Zview, Scribner Associates Inc., 2005.
10. Ullmann, H., Trofimenko, N., Tietz, F., Stöver, D. and Ahmad-Khanlou, A., Correlation between thermal expansion and oxide ion transport in mixed conducting perovskite-type oxides for SOFC cathodes. *Solid State Ionics*, 2000, **138**, 79–90.
11. Steele, B. C. H., Behaviour of porous cathodes in high temperature fuel cells. *Solid State Ionics*, 1997, **94**, 239–248.
12. Adler, S. B., Mechanism and kinetics of oxygen reduction on porous $La_{1-x}Sr_xCoO_{3-\delta}$ electrodes. *Solid State Ionics*, 1998, **111**, 125–134.
13. Adler, S. B., Limitations of charge-transfer models for mixed-conducting oxygen electrodes. *Solid State Ionics*, 2000, **135**, 603–612.
14. Adler, S. B., Lane, J. A. and Steele, B. C. H., Electrode kinetics of porous mixed-conducting oxygen electrodes. *J. Electrochem. Soc.*, 1996, **143**, 3554–3564.
15. Mauvy, F., Lalanne, C., Bassat, J. M., Grenier, J. C., Zhao, H., Huo, L. and Stevens, P., Electrode properties of Ln_2NiO_{4+d} (Ln = La, Nd, Pr) AC impedance and DC polarization studies. *J. Electrochem. Soc.*, 2006, **153**, A1547–A1553.
16. Dyck, C. R., Yu, Z. B. H. and Krstic, V. D., Thermal expansion matching of $Gd_{1-x}Sr_xCoO_{3-\delta}$ composite cathodes to $Ce_{0.8}Gd_{0.2}O_{1.95}$ IT-SOFC electrolytes. *Solid State Ionics*, 2004, **171**, 17–23.

17. Qiang, F., Sun, K., Zhang, N., Zhu, X. D., Le, S. and Zhou, D., Characterization of electrical properties of GDC doped A-site deficient LSCF based composite cathode using impedance spectroscopy. *J. Power Sources*, 2007, **168**, 338–345.
18. Jorgensen, M., Primdhal, S. and Mogensen, M., Characterization of composite SOFC cathodes using electrochemical impedance spectroscopy. *Electrochim. Acta*, 1999, **44**, 4195–4201.
19. Hagiwara, A., Hobara, N., Takizawa, K., Sato, K., Abe, H. and Naito, M., Microstructure control of SOFC cathodes using the self-organizing behavior of LSM/ScSZ composite powder material prepared by spray pyrolysis. *Solid State Ionics*, 2007, **178**, 1123–1134.
20. Zhu, X. D., Sun, K. N., Zhang, N. Q., Chen, X. B., Wu, L. J. and Jia, D. C., Improved electrochemical performance of $SrCo_{0.8}Fe_{0.2}O_{3-\delta}$–$La_{0.45}Ce_{0.55}O_{2-\delta}$ composite cathodes for IT-SOFC. *Electrochem. Commun.*, 2007, **9**, 431–435.
21. Fu, C., Sun, K., Zhang, N., Chen, X. and Zhou, D., Electrochemical characteristics of LSCF-SDC composite cathode for intermediate temperature SOFC. *Electrochim. Acta*, 2007, **52**, 4589–4594.
22. Dusastre, V. and Kilner, J. A., Optimisation of composite cathodes for intermediate temperature SOFC applications. *Solid State Ionics*, 1999, **126**, 163–174.
23. Hagiwara, A., Hobara, N., Takizawa, K., Sato, K., Abe, H. and Naito, M., Preparation and evaluation of mechanochemically fabricated LSM/ScSZ composite materials for SOFC cathodes. *Solid State Ionics*, 2006, **177**, 2967–2977.
24. Bebelis, S., Kotsionopoulos, N., Mai, A., Rutenbeck, D. and Tiez, F., Electrochemical characterization of mixed conducting and composite SOFC cathodes. *Solid State Ionics*, 2006, **177**, 1843–1848.
25. Colomer, M. T., Steele, B. C. H. and Kilner, J. A., Structural and electrochemical properties of the $Sr_{0.8}Ce_{0.1}Fe_{0.7}Co_{0.3}O_{3-\delta}$ perovskite as cathode material for ITSOFCs. *Solid State Ionics*, 2002, **147**, 41–48.
26. Takeda, Y., Kanno, R., Noda, M., Tomida, Y. and Yamamoto, O., Cathodic polarization phenomena of perovskite oxide electrodes with stabilized zirconia. *J. Electrochem. Soc.*, 1987, **134**, 2656–2661.